

# Wavelet-Based Convolutional Neural Network for Parkinson's Disease Detection in Resting-State Electroencephalography

S. Cahoon, F. Khan, M. Polk and M. Shaban

Electrical and Computer Engineering, University of South Alabama, Mobile, Alabama, USA  
{sec1721, ffk1821, mcp1721}@jagmail.southalabama.edu, mshaban@southalabama.edu

**Abstract**— Electroencephalography (EEG) is not commonly used for Parkinson's Disease (PD) detection and diagnosis. However, it has been recently indicated in the literature that EEG may present unique biomarkers and features of the disease. In the current study, we introduce a Convolutional Neural Network (CNN) framework that exploits the wavelet domain of resting-state EEG in order to classify subjects into PD and Healthy Controls (HC). It was observed that PD exhibits a continuous uniform fading of the low wavelet scales as compared with HC. In addition, the proposed CNN approach was able to detect PD with a 4-fold as well as 10-fold cross-validation performance of up to 99.9% surpassing the-state-of-the-art deep learning-based architectures.

## I. INTRODUCTION

Parkinson's disease (PD) [1] is a progressive neurodegenerative disorder with serious complications representing the fourteenth cause of death in the United States. Symptoms may include hand tremors, bradykinesia, limb rigidity, gait and balance problems, speech and sleep behavior disorders. Clinical diagnosis is considered the gold standard for assessment of the disease. Meanwhile, there are no established biomarkers of PD that can monitor the progression to advanced stages or assess medication response.

Although electroencephalography (EEG) is not a diagnostic test for PD, it has been recently shown that subjects with PD exhibit reduced beta and gamma powers [2-4], and significant phase-amplitude coupling changes as compared to healthy controls (HC) [5] [6].

Machine and deep learning techniques (MDL) were recently used to exploit the unique features of EEG and detect PD [7-13]. The aforementioned techniques provided a performance that ranges from 88% to 98%. However, most of the reported methods did not provide further insights into sensitivity, specificity, and weighted Kappa score which reveals sufficient information on the reliability of the methods.

In this paper, we propose an accurate and sensitive MDL approach that exploits the wavelet domain of resting-state EEG that was previously recorded for PD subjects and HC. The deep-learning approach achieves a significantly higher accuracy with respect to the-state-of-the-art approaches presented [7-13] for classifying subjects into HC and PD. Therefore, we offer a novel precise computer aided-diagnostic tool that is capable of pre-screening patients prior to the traditional clinical diagnosis.

## II. MACHINE AND DEEP LEARNING FOR PD DETECTION BASED ON EEG

MDL techniques are algorithms that extract handcrafted or learned features from structured or unstructured data and then classify the data based on the features. These algorithms are generally classified into supervised and unsupervised approaches. Supervised approaches require human supervision during the training process of the model by providing adequate labeled data. These techniques are mainly used for classification and regression purposes, and their performance relies on the size of the dataset. Examples of supervised learning are support vector machines (SVM), decision trees, artificial neural networks (ANNs), convolutional neural networks (CNNs), and recurrent neural networks (RNNs).

Unsupervised approaches provide an approximate representation for an underlying data structure to extract further information about the data. In this case, training of the models is usually achieved using unlabeled data to cluster the data into groups or create association rules that better describe the data. Examples include K-Means clustering, autoencoders, deep belief networks and self-organizing maps. Four popular learning architectures (i.e., ANNs, CNNs, Autoencoders, and RNNs) are extensively used in medical data applications.

Several studies have proposed the use of MDL techniques on the promising EEG modality to distinguish between HC and subjects with PD [7-13]. Vanegas et al. introduced the use of extra trees, linear regression, and decision tree classifiers to identify EEG-based biomarkers of PD with an area under the curve (AUC) of 99.4%, 94.9%, and 86.2% respectively [7]. Wagh et al. proposed a graph CNN to classify various neurological diseases including PD with an accuracy of 85% [8]. Koch et al. developed a random forest classifier to detect PD based on clinical and automated features from the EEG data with an AUC of 91% [9]. Oh et al. used 13-layer CNN to detect de novo PD subjects with an accuracy of 88.3% [10]. Shit et al. and S. Lee et al. proposed hybrid CNN-RNN models to detect PD from EEG data with an accuracy of 82.9% and 96.9% respectively [11] [12]. In [13], the author proposed an ANN-based framework to screen subjects into PD and HC with an accuracy of 98.

## III. PROPOSED WAVELET-BASED CNN METHOD

### A. EEG Dataset

We have acquired the latest version of an EEG dataset (i.e., 1.0.4) for subjects with PD and HC via

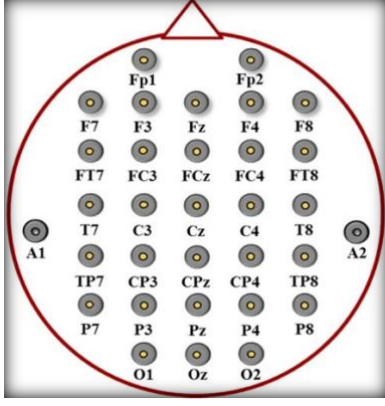


Figure 1. Locations of 32-EEG electrodes

OpenNeuro [14]. The dataset was originally collected at the Aron lab at the University of California at San Diego for 15 right-handed PD patients recruited from the Scripps Clinic in La Jolla, California with mild or moderate disease stage and 16 matched HC. The EEG data were captured using thirty-two standard electrodes (See Fig. 1) and sampled at a rate of 512 S/s.

### B. Proposed Framework

In the first stage, the EEG signal  $x(t)$  measured by the  $i^{\text{th}}$  electrode was transformed into the Wavelet domain using the Continuous Wavelet Transform (CWT) defined as follows:

$$X_i(s, \tau) = \frac{1}{\sqrt{s}} \int_0^\infty x_i(t) \psi\left(\frac{t-\tau}{s}\right) dt \quad (1)$$

where  $\psi$  is the Morlet analysis wavelet,  $\tau$  and  $s$  are the time shift and the scale of the wavelet respectively. The scale is inversely proportional to the Fourier frequency where smaller scales correspond to higher frequencies.

Further, the absolute values of the wavelets  $X_i(s, \tau)$  after being scaled up by a factor of 100 were generated for each EEG signal. The values have an approximate

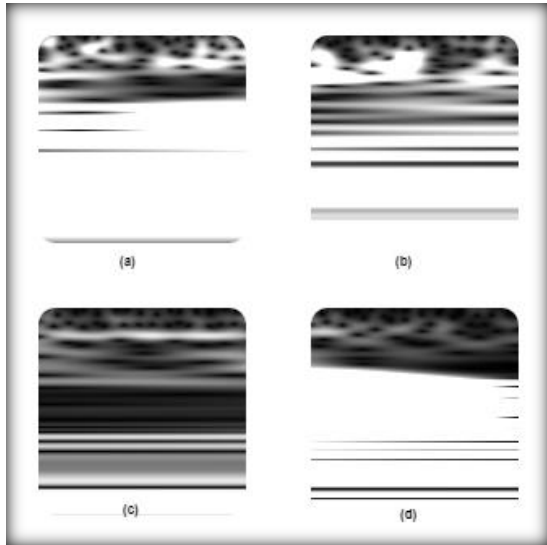


Figure 2. Scalogram of the EEG wavelet transform for (a) (b) HC and (c) (d) PD

dimension of  $138 \times 96,768$  for HC and  $138 \times 97,792$  for PD. Further, these values were then segmented in time into  $128 \times 128$  samples where 128 scales were selected out of 138 scales (i.e. only the highest 10 scales or the lowest 10 Fourier frequencies were discarded). Examples of the Morlet wavelets of EEG signals recorded by the first channel for HC and PD are shown in Fig. 2. We have noticed that there was a continuous uniform deterioration in the wavelet domain for PD subjects when compared with HC especially at lower scales (i.e., higher frequencies). This was represented as a dark shade in the PD wavelets while there were spontaneous white spots in the wavelets for HC within the low-scale interval.

Further, the second stage utilizes a 20-layer CNN that we have recently proposed and tested in a computer vision application (i.e., detection of oil spill from satellite aperture radar images) [15]. The structure of the proposed CNN is described in Table 1. The proposed network consists of 20 layers of convolutions, rectified linear units (ReLU), and maximum pooling (MaxPooling). In addition, the input layer hosts the gray-scale wavelet images while the output layer determines the SoftMax probabilities and classifies the images using an appropriate threshold. Fig. 3 describes the main stages of the proposed framework.

The ability of the CNN to classify the EEG samples was assessed via estimating the accuracy, sensitivity, specificity, AUC of ROC, and Kappa score of the model on 4-fold and 10-fold cross validated data.

The weighted Kappa score ( $Q$ ) ensures that any agreements between the predictions and the ground truth did not occur by chance, therefore it was used to verify the reliability of the decisions provided by the model.  $Q$  is defined as follows:

$$Q = 1 - \frac{\sum_{m=0}^2 \sum_{n=0}^2 g(m,n) f(m,n)}{\sum_{m=0}^2 \sum_{n=0}^2 g(m,n) o(m,n)} \quad (2)$$

where  $f(m,n)$  is an element of the normalized confusion matrix,  $o(m,n)$  is an entry of the outer product matrix of predicted and actual labels histograms and  $g(m,n)$  is calculated using the following equation:

$$g(m,n) = m - n. \quad (3)$$

## IV. EXPERIMENTAL DESIGN AND ANALYSIS

A total of 24,264 wavelet images of a dimension  $128 \times 128$  were generated from the EEG time-series data for each spatial channel (i.e. channels 1 to 32) with 12,260 images considered for the sixteen HC and 12,004 identified for the fifteen PD subjects. The proposed CNN described in Table 1 was then trained on the images for 40 epochs using the backpropagation algorithm. The number of images processed at a single time was 50 while the learning rate of  $10^{-5}$  was adopted. In this study, we have used both the 4-fold and 10-fold cross-validation techniques to test the CNN model.

Table 1. CNN Structure

Layer	No. of Layers	Layer Size	No. of Feature Maps
Image	1	$128 \times 128$	-
Convolution	4	$11 \times 11$	32
MaxPooling	1	$2 \times 2$	32
Convolution	4	$9 \times 9$	64
MaxPooling	1	$2 \times 2$	64
Convolution	4	$7 \times 7$	128
MaxPooling	1	$2 \times 2$	128
Dense	4	128, 64, 32, 16	-
Classification	1	2	-

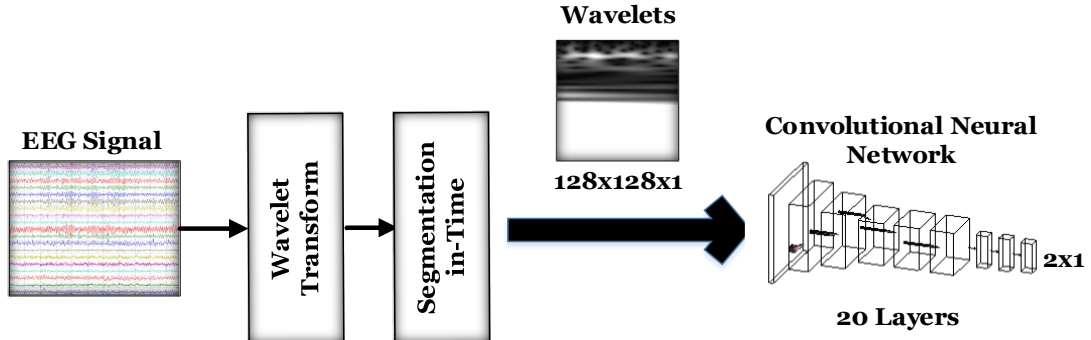


Figure 3. Proposed wavelet-based CNN approach

For instance, in the 4-fold cross validation, three-fourth of the dataset was used for training the model while the rest of the dataset was reserved for validation and performance evaluation. Accordingly, we ensured that there was no overlap or reuse among the training and validation samples. The mean training, validation accuracy, sensitivity, specificity, Kappa score, and AUC were measured (see Table 2 and Table 3) for four randomly selected channels (i.e., Fp1, FC1, CP5 and Fz). Based on Table 2 and Table 3, the validation accuracy ranges from 98.6% to 99.9% for the four selected channels. The sensitivity varies from 98.6%

to 99.9% while specificity changes from 98.3% to 99.9% as well.

The Kappa score maintained a high level that was almost above 0.97 justifying the reliability of the performance results obtained and showing the very limited bias of the proposed model. In addition, the ROC graphs for the 4-fold cross-validation classifier across the four selected channels are presented in Fig. 4. Evidently, the proposed classifier possesses a very high separability between PD and HC at the four different channels.

In summary, the proposed approach achieved a best-case accuracy of almost 99.9% (i.e. a consistent accuracy for both cross-validation methods) at CP5 outperforming the-state-of-the-art architectures utilizing CNN [10], hybrid CNN-RNN [11] [12] and ANN [13] to detect or screen PD subjects (see

Table 2. 4-Fold Cross Validation Results

Channel	Fp1	FC1	CP5	Fz
Training Accuracy	100%	100%	100%	100%
Validation Accuracy	98.6%	99.7%	99.9%	98.9%
Sensitivity	98.9%	99.8%	99.9%	99.1%
Specificity	98.3%	99.6%	99.9%	98.8%
Weighted Kappa	0.97	0.99	0.99	0.98
AUC	0.99	0.99	0.99	0.99

Table 3. 10-Fold Cross Validation Results

Channel	Fp1	FC1	CP5	Fz
Training Accuracy	100%	100%	100%	100%
Validation Accuracy	98.7%	99.8%	99.9%	98.9%
Sensitivity	98.6%	99.8%	99.9%	98.8%
Specificity	98.7%	99.8%	99.9%	98.9%
Weighted Kappa	0.97	0.99	0.99	0.97
AUC	0.97	0.98	0.99	0.99

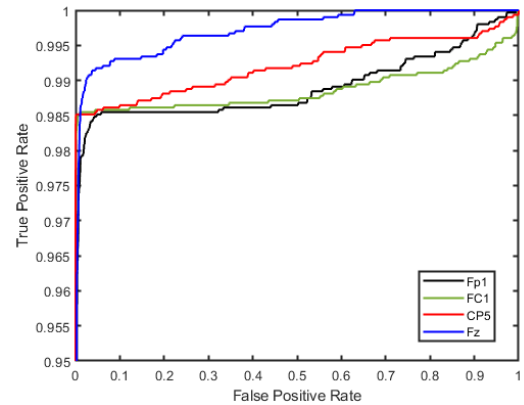


Figure 4. ROC of the proposed approach for the four selected channels

Table 4. Accuracy Comparison of Our Approach Related Work Used for PD Detection

Method	Proposed	[10]	[11]	[12]	[13]
Accuracy	99.9%	88%	83%	93%	98%

Table 4). Accordingly, the proposed approach provides a promising PD screening initiative that exploits the wavelet domain of EEG signals offering a very high accuracy, sensitivity, and specificity computer-aided diagnostic tool that can support physicians to provide an objective, and reliable assessment of the disease.

## V. SUMMARY

In this work, we have developed a deep-learning mechanism that exploits the wavelet domain of resting-state EEG signals to detect PD. The proposed approach consists of three stages; a Morlet wavelet transformation, time segmentation, CNN feature extraction and classification. It was observed that subjects with PD exhibit uniform dark regions corresponding to the low-scale wavelet components as compared with HC. Due to the discrepancies arising between HC and PD in the wavelet domain, a proposed CNN structure was able to efficiently discriminate between the EEG recordings corresponding to PD and HC where 4-fold as well as 10-fold cross-validation accuracy, sensitivity, and specificity reached up to 99.9% at CP5.

A minimum weighted Kappa score of 0.97 was attained at the Fp1 electrode providing a piece of evidence on the robustness of the proposed technique as well as confidence in the ability of the technique to detect PD. When compared with the 13-layer CNN used in [10], the hybrid CNN-RNN of [11], the hybrid CNN-LSTM deployed in [12] and our prior work utilizing an ANN framework [13], we have introduced an efficient low-complexity design that used the powerful capabilities of CNN for feature extraction and classification to exploit the insufficiently investigated wavelet EEG domain for PD detection and screening. The proposed wavelet CNN-based approach can serve as a tool for neurologists to provide an objective as well as accurate prediction of the disease status.

Although the proposed approach successfully detects PD based on resting-state EEG, it may not be suitable to support the pre-clinical diagnosis of the disease since the approach has been trained and validated on recorded EEG for patients with a confirmed clinical diagnosis of PD. To address this challenge, we plan to develop an AI framework based upon a sleep EEG dataset acquired for subjects who were later diagnosed with PD as well as visualize the features detected by this AI framework. This may provide further insights on critical and unique early EEG biomarkers of the disease since it has been shown in the literature that prodromal PD (i.e., early stage PD) subjects usually

present with sleep disorders and reduction in rapid eye movement (REM) sleep [16]. Further, due to the limited number of subjects per each disease stage, we were not able to validate the approach to further classify the subjects based on the progression of the disease. Having access to larger and more diverse datasets will allow a successful and reliable application of AI for PD screening and staging.

## ACKNOWLEDGEMENTS

Partial support of this research was provided by the Woodrow W. Everett, Jr. SCEE Development Fund in cooperation with the Southeastern Association of Electrical Engineering Department Heads.

## REFERENCES

- [1] W. Dauer, and S. Przedborski, "Parkinson's disease: mechanisms, and models," *Neuron*, vol. 39, no. 6, pp. 889-909, 2003.
- [2] L. Pezard, R. Jech, and E. Ruzicka, "Investigation of non-linear properties of multichannel EEG in the early stages of Parkinson's disease," *Clinical Neurophysiology*, vol. 165, no. 1, pp. 38-45, 2001.
- [3] J. Bosboom, D. Stoffers, C. Stam, B. Dijk, et al., "Resting state oscillatory brain dynamics in Parkinson's disease: an MEG study," *Clinical Neurophysiology*, vol. 117, no. 11, pp. 2521-2531, 2006.
- [4] R. Soikkeli, J. Partanen, H. Soininen, A. Pääkkönen, and P. Riekkinen, "Slowing of EEG in Parkinson's disease," *Electroencephalography, and Clinical Neurophysiology*, vol. 79, no. 3, pp. 159-165, 1991.
- [5] C. Hemptinne, E. Ryapolova-Webb, E. Air, P. Garcia, et al., "Exaggerated phase-amplitude coupling in the primary motor cortex in Parkinson disease," in *Proceedings of National Academy of Sciences of the United States of America*, vol. 110, pp. 4780-4785, 2013.
- [6] N. Swann, C. Hemptinne, A. Aron, J. Ostrem, et al., "Elevated synchrony in Parkinson disease detected with electroencephalography," *Annals of Neurology*, vol. 78, pp. 742-750, 2015.
- [7] M. Vanegas, M. Ghilardi, S. Kelly, and A. Blangero, "Machine Learning for EEG-Based Biomarkers in Parkinson's Disease," in *IEEE International Conference on Bioinformatics and Biomedicine*, Madrid, Spain, 2018.
- [8] N. Wagh, and Y. Varatharajah, "EEG-GCNN: Augmenting Electroencephalogram-Based Neurological Disease Diagnosis Using a Domain-Guided Graph Convolutional Neural Network," *Machine Learning Research*, vol. 136, pp. 367-378, 2020.
- [9] M. Koch, V. Geraedts, et al., "Automated Machine Learning for EEG-Based Classification of Parkinson's Disease Patients," in *IEEE International Conference on Big Data*, Los Angeles, USA, 2019.
- [10] S. Oh, Y. Hagiwara, U. Raghavendra, et al., "A deep learning approach for Parkinson's disease diagnosis from EEG signals," *Neural Computing and Applications*, vol. 32, pp. 10927-10933, 2020.
- [11] X. Shi, T. Wang, et al., "Hybrid Convolutional Recurrent Neural Networks Outperform CNN and RNN in Task-State EEG Detection for Parkinson's Disease," in *Asia-Pacific Signal and Information Processing Association Annual Summit and Conference*, Lanzhou, China, 2019.
- [12] S. Lee, R. Hussein, and M. McKeown, "A Deep Convolutional-Recurrent Neural Network Architecture for Parkinson's Disease EEG Classification," in *IEEE Global Conference on Signal and Information Processing*, Ottawa, Canada, 2019.
- [13] M. Shaban, "Automated Screening of Parkinson's Disease Using Deep Learning Based Electroencephalography," in

International IEEE EMBS Conference on Neural Engineering, Virtual, 2021.

- [14] A. Rockhill, N. Jackson, et al., "UC San Diego Resting State EEG Data from Patients with Parkinson's Disease," 2020. [Online]. Available: <https://openneuro.org/datasets/ds002778/versions/1.0.4>.
- [15] M. Shaban, R. Salim, H. Abu Khalifeh, et al., "A Deep-Learning Framework for the Detection of Oil Spills from SAR Data," *Sensors*, MDPI, vol. 21, no. 7, 2021.
- [16] L. Chahine, A. Amara, and A. Videnovic, "A systematic review of the literature on disorders of sleep and wakefulness in Parkinson's disease from 2005 to 2015," *Sleep Medicine Reviews*, vol. 35, pp. 33-50, 2017.